

# Nuclear spin singlet states as a contrast mechanism for NMR spectroscopy

Stephen J. DeVience<sup>a\*</sup>, Ronald L. Walsworth<sup>b,c,d</sup> and Matthew S. Rosen<sup>d,e,f</sup>



Nuclear magnetic resonance (NMR) spectra of complex chemical mixtures often contain unresolved or hidden spectral components, especially when strong background signals overlap weaker peaks. In this article we demonstrate a quantum filter utilizing nuclear spin singlet states, which allows undesired NMR spectral background to be removed and target spectral peaks to be uncovered. The quantum filter is implemented by creating a nuclear spin singlet state with spin quantum numbers  $j=0, m_z=0$  in a target molecule, applying a continuous RF field to both preserve the singlet state and saturate the magnetization of undesired molecules and then mapping the target molecule singlet state back into an NMR observable state so that its spectrum can be read out unambiguously. The preparation of the target singlet state can be carefully controlled with pulse sequence parameters, so that spectral contrast can be achieved between molecules with very similar structures. We name this NMR contrast mechanism 'Suppression of Undesired Chemicals using Contrast-Enhancing Singlet States' (SUCCESS) and we demonstrate it *in vitro* for three target molecules relevant to neuroscience: aspartate, threonine and glutamine. Copyright © 2013 John Wiley & Sons, Ltd.

Supporting information may be found in the online version of this paper.

**Keywords:** quantum filter; nuclear spin singlet state; glutamine; spin locking

## INTRODUCTION

Nuclear magnetic resonance (NMR) spectroscopy provides a quantitative, non-destructive measure of chemical concentrations in complex mixtures both *in vitro* and *in vivo*. In many cases, the spectral lines are narrow while the range of resonance frequencies is broad, resulting in little overlap of spectral components. However, in mixtures of biomolecules, such as blood, urine and brain tissue, strong and broad NMR spectra from a few dominant metabolites often overlap and hence obscure NMR spectra with weaker intensities from species of interest at low concentration (1–5). Furthermore, some abundant metabolites, such as glutamine and glutamate, have such similar structures that their NMR spectra are nearly identical and are difficult to resolve. In both these situations, signal averaging is generally not able to improve the resolution of chemical component identification.

While improved spectral resolution can be achieved using higher magnetic-field instruments, this is often a costly solution, especially for magnetic resonance spectroscopy (MRS) applications. The simplest approach for resolving overlapping signals is spectral deconvolution, but this requires *a priori* knowledge of the line shape, which can change depending on sample conditions and shimming. A better approach is to distinguish molecules further by their intramolecular magnetic couplings by acquiring a two-dimensional spectrum. However, a large number of scans is required to acquire a spectrum in the second dimension. An alternative approach relies on quantum filters to remove undesired spectral components and to select those of interest. Quantum filtration works by creating a quantum coherence in a target spin system and then applying phase cycling or gradient filters to selectively pass or suppress the coherences from the target (6). The technique utilizes the same intramolecular magnetic couplings measured in a multidimensional spectrum, while utilizing only one set of

evolution times. The goal is to remove overlapping signals as much as possible to minimize the contribution of other species to the spectral lines of interest. Common applications include water and fat suppression as well as metabolite-specific contrast enhancement in MRS, amino-acid-specific contrast

\* Correspondence to: S. J. DeVience, Harvard-Smithsonian Center for Astrophysics, MS 59, 60 Garden St, Cambridge, MA 02138, USA.  
E-mail: devience@fas.harvard.edu

a S. J. DeVience  
Department of Chemistry and Chemical Biology, Harvard University, 12 Oxford St, Cambridge, MA, 02138, USA

b R. L. Walsworth  
Harvard-Smithsonian Center for Astrophysics, 60 Garden St, Cambridge, MA, 02138, USA

c R. L. Walsworth  
Center for Brain Science, Harvard University, 52 Oxford St, Cambridge, Massachusetts, 02138, USA

d R. L. Walsworth, M. S. Rosen  
Department of Physics, Harvard University, 17 Oxford St, Cambridge, MA, 02138, USA

e M. S. Rosen  
Harvard Medical School, 25 Shattuck Street, Boston, MA, 02115, USA

f M. S. Rosen  
A. A. Martinos Center for Biomedical Imaging, 149 Thirteenth St, Suite 2301, Charlestown, MA, 02129, USA

**Abbreviations:** Asp, aspartate; DQ, double quantum; Gln, glutamine; Glu, glutamate; NAA, N-acetylaspartate; SAR, specific absorption rate; SNR, signal-to-noise ratio; SUCCESS, Suppression of Undesired Chemicals using Contrast-Enhancing Singlet States; Thr, threonine;  $T_1$ , singlet lifetime; ZQ, zero quantum;  $\nu_{rf}$ , spin-lock nutation frequency.

enhancement in protein spectroscopy and metabolic analysis of blood and urine (7–17). However, these quantum filters have had limited success in differentiating the signals of similarly structured molecules where the chemical shifts and coupling parameters are nearly identical (18,19).

In this work, we demonstrate a new type of quantum filter known as ‘Suppression of Undesired Chemicals using Contrast-Enhancing Singlet States’ (SUCCESS). In this technique, we create and select nuclear spin singlet states in pairs of coupled protons or pairs of coupled methylene groups. The multi-pulse sequence required to create, preserve and measure the target singlet state produces strong contrast relative to undesired spectral components even when the spectra of two molecules (target and undesired) nearly overlap. SUCCESS also produces excellent suppression of signals from spins in which no singlet state can be created.

Existing quantum filters utilize coherences comprised of spin quantum states projected along the z-axis, i.e. the levels of  $m_z$  (6). For example, a double-quantum filter selects (or rejects) all double quantum coherences, which consist of two or more spins in an  $m_z = 1$  state. However, for strongly coupled systems, in which the coupling between nuclei is much stronger than the difference between their resonance frequencies, it is more appropriate to describe the eigenstates by their total spin quantum number,  $j$ . One example is the  $H_2$  molecule, in which nuclear spin states cannot be properly described by Zeeman eigenstates of the individual spins (20) but are instead combined to form new states classified as spin singlet and triplet (not to be confused with singlets and triplets in spectroscopic notation describing peak structure). This results in two species of hydrogen molecules: *para*- $H_2$ , with  $j = 0$  and the spin singlet eigenstate  $|S_0\rangle = (|\uparrow\downarrow\rangle - |\downarrow\uparrow\rangle)/\sqrt{2}$ ; and *ortho*- $H_2$ , with  $j = 1$  and spin triplet eigenstates  $|T_-\rangle = |\uparrow\uparrow\rangle$ ,  $|T_0\rangle = (|\uparrow\downarrow\rangle + |\downarrow\uparrow\rangle)/\sqrt{2}$ , and  $|T_+\rangle = |\downarrow\downarrow\rangle$  (20). In our notation  $\uparrow$  represents a spin aligned with the applied magnetic field  $B_0$  while  $\downarrow$  represents a spin that is anti-aligned.

Recent work has shown that, even when spins are only weakly coupled naturally, spin singlet and triplet states can be created by applying a continuous RF spin-locking field on-resonance with the spins so that their resonance-frequency differences are suppressed (21–23). Singlet states produced this way in a variety of molecules often exhibit lifetimes many times longer than the spin–lattice relaxation time,  $T_1$ , as a result of the state’s unique symmetry properties (24–31). These long-lived singlets have been used to measure exchange and dynamics on slow timescales that were previously inaccessible (32–34) and to store polarization beyond conventional relaxation times (35,29). Most singlet-state experiments have used specially designed or selected molecules to produce singlet-state lifetimes as long as possible, but the singlet state can actually be prepared in nearly any coupled pair of spin-1/2 nuclei. In many cases, surrounding spins and other couplings will perturb the singlet state and cause it to relax on a timescale of  $1/T_1$  or faster, but within this timeframe the nuclear spin singlet state exists as a unique spin population that can be preserved and used as a resource for quantum filtration.

In the SUCCESS technique, we use continuous RF spin locking, which simultaneously drives triplet states and other uncoupled spins to saturation more quickly than  $T_1$ . We utilize this feature as a contrast mechanism in the basic SUCCESS pulse sequence shown in Figure 1A, which consists of three steps.

- (1) Prepare target nuclear spins in a singlet state, while minimizing the singlet character of any other groups of spin.

These singlets might be prepared on a specific molecule in a mixture or a specific group in a larger molecule.

- (2) Apply a resonant RF spin-locking field to preserve the singlet state and drive all other spin states to saturation.
- (3) Convert the target singlet population back into transverse magnetization for readout. The resulting NMR spectrum should then consist only of contributions from the target spins that were prepared in a singlet state.

In real systems, the applied RF field contains a limited power across a limited bandwidth, so that saturation of the background spin systems is often incomplete. Background suppression can be improved using a polyhedral, spherically symmetric phase cycle developed by Pileio *et al.*, which passes the spherically symmetric singlet state but removes all other signals (36). The addition of phase cycling results in the optimized SUCCESS sequence shown in Figure 1B. The highest coherence order removed by the phase cycle depends on the number of steps chosen: the closer one approximates a sphere, the better one isolates the singlet. In the  $^1H$  NMR demonstration experiments presented below, we chose a 24-step cycle that removes states up to  $j = 3$ , which is sufficient for background molecules with up to six protons.

Background molecules may also contain spin groups capable of producing singlet states and with spectral components overlapping the target. Fortunately, the efficient preparation of a singlet state requires a pulse sequence with three properly chosen delays that depend on the scalar coupling and chemical shifts of each molecule. We find that, through careful selection of these delays, a singlet can be created in the target molecule only. For example, the simulation results shown in Figure 1C and 1D show that, by properly selecting delays  $\tau_2$  and  $\tau_3$ , large singlet-state magnetization can be produced in aspartate while minimal singlet-state magnetization is produced in N-acetylaspartate.

## EXPERIMENTAL

We demonstrated the SUCCESS technique *in vitro* on three target molecules that are important brain metabolites: aspartate, threonine and glutamine. The spectral lines of these molecules are overlapped by peaks from N-acetylaspartate, *myo*-inositol and glutamate, respectively. The test mixtures we employed are listed in Table 1.

Each consisted of a target molecule and the interfering background substance dissolved in a pH 7.0 phosphate buffer with 69 mM total phosphate concentration. Metabolite concentrations were chosen to reflect typical ratios found *in vivo* but at higher absolute concentration. We also created a control solution for each target and background molecule alone in the pH 7.0 phosphate buffer. Reagents were purchased from Sigma Aldrich, St. Louis, MO.

We obtained  $^1H$  NMR spectra using a Bruker 4.7 T vertical bore spectrometer with a 10-mm diameter probe. Data were collected with XWINNMR software running on a Silicon Graphics  $O_2$  computer. A transmitter power of 100 W required a  $90^\circ$  pulse length of 26  $\mu s$  and a  $180^\circ$  pulse length of 46  $\mu s$ . Exponential apodization was applied to all spectra with either 0.5 Hz or 1.0 Hz line-broadening constants. Spectra of the mixtures and controls were first obtained with a ‘one-pulse’ sequence by applying a  $90^\circ$  pulse and acquiring an FID. Spin–lattice relaxation times of the molecules were measured in control solutions using an inversion recovery sequence. We then used measured  $J$ -couplings and peak positions of each molecule to calculate

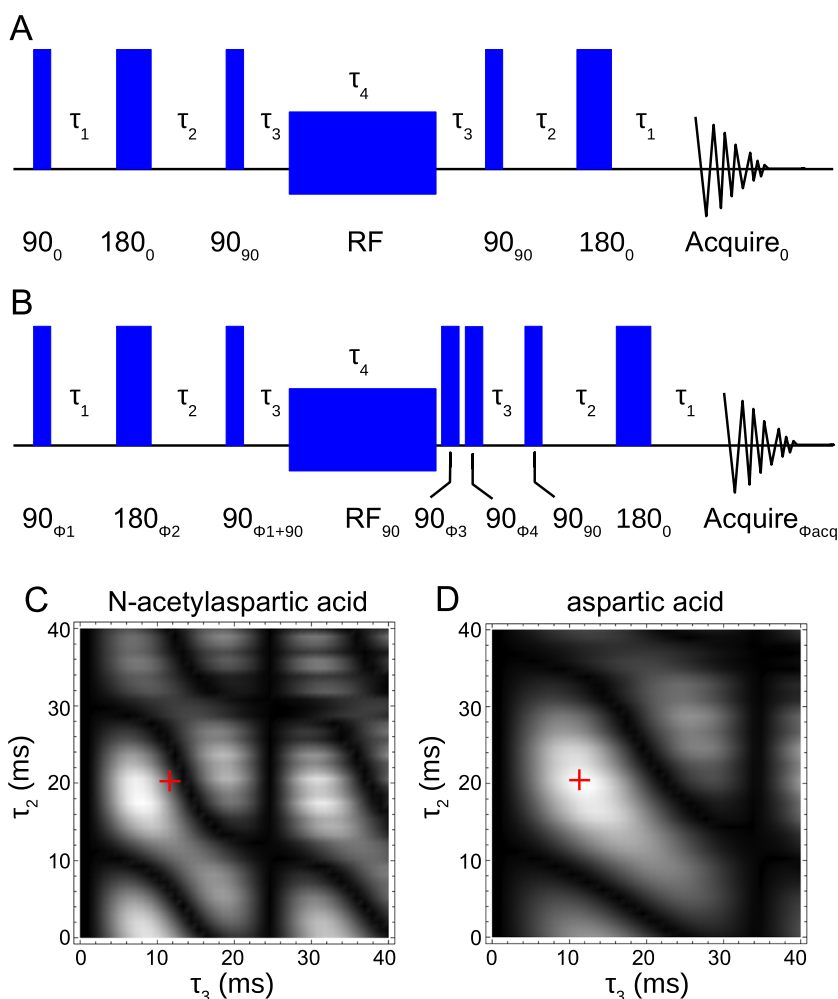


**Figure 1.** (A) **Basic SUCCESS pulse sequence.** The NMR transmitter frequency,  $\nu_0$  (chemical shift  $\delta_0$ ), is placed at the average resonance frequency of the two target nuclear spins at a chemical shift  $\delta_{av}$ . Three pulses, with corresponding delays  $\tau_1$ ,  $\tau_2$  and  $\tau_3$ , create a population difference between singlet and triplet states on the target spins, described by the density matrix  $\rho_{ST} = |S_0\rangle\langle S_0| - |T_0\rangle\langle T_0|$ . Continuous RF spin locking, also applied at the average resonance frequency of the target spins for time  $\tau_4$ , preserves the singlet state while driving other states toward saturation. Finally, two of the first three pulses are repeated in reverse order to return the remaining singlet population into transverse magnetization for readout. (B) **Optimized SUCCESS pulse sequence.** To improve the suppression of non-singlet states, two filtering pulses are added as part of a spherically symmetric phase cycle. (C) and (D) Simulated NMR signal intensity maps for N-acetylaspartic acid and aspartic acid, which show that pulse sequence delays can be chosen to produce the singlet state selectively in one molecule and not in the other. The red cross marks the parameters used in the demonstration in which aspartic acid was targeted. Parameters were chosen as a compromise between signal intensity and strong contrast. Higher contrast can be achieved with slightly longer values of  $\tau_2$  and  $\tau_3$ , but with lower target signal intensity.

**Table 1.** Target and background concentrations used in the SUCCESS demonstrations

Target	Conc. (mM)	Background	Conc. (mM)
Aspartic acid	3.0	N-acetylaspartic acid	11.4
Threonine	50.0	<i>myo</i> -Inositol	50.0
Threonine	5.0	<i>myo</i> -Inositol	50.0
Glutamine	40.0	Monosodium glutamate	80.0

optimal delays  $\tau_1$ ,  $\tau_2$  and  $\tau_3$  for the target spins by simulating the spin system with the Mathematica package *SpinDynamica* (37) and adjusting delays to maximize singlet-state creation in the target and minimize singlet-state creation in the background. For example, the simulation results shown in Figure 1C and 1D

demonstrate that, by properly selecting  $\tau_2$  and  $\tau_3$ , large singlet-state magnetization can be produced in aspartate while little singlet state is produced in N-acetylaspartate. Singlet lifetimes were measured in the controls using the SUCCESS sequence in Figure 1B by varying the relaxation delay  $\tau_4$ . During  $\tau_4$ , spin locking was performed with a spin-lock nutation rate  $\nu_n$  such that  $\nu_n > 5\Delta\nu$ , where  $\Delta\nu$  is the chemical shift splitting between the two target peaks. The 24-step phase cycle was used with parameters given in Supplementary Table S1. For both one-pulse and SUCCESS experiments, a delay of  $5T_1$  was used between each scan to allow maximal recovery of magnetization. SUCCESS spectra of each mixture were acquired and the delays were optimized experimentally to produce the best contrast enhancement for the target molecule. Identical SUCCESS spectra were acquired for control solutions. We normalized each spectrum by dividing by the number of scans,  $N$ , so that the signal intensity per scan could be compared. More scans were used

for SUCCESS experiments so that a sufficient signal-to-noise ratio (SNR) could be achieved for proper comparison with the one-pulse experiments. A large number of scans (of the order of thousands) was needed to achieve high SNR of the low-concentration solutions because of the low sensitivity of the 200-MHz spectrometer.

We quantified the effectiveness of the SUCCESS quantum filter in terms of the contrast enhancement of the target molecule's spectral peaks: i.e. the ratio

$$CE = \frac{C_S}{C_R}, \quad [1]$$

where  $C_R$  is the contrast from a one-pulse experiment and  $C_S$  is the contrast from a SUCCESS experiment. The contrast can be defined in two ways, using either (i) the peak intensities per scan of individual target spectral lines relative to the interfering background (undesired molecule) peak intensity per scan (we call this the peak contrast) or (ii) the integrated intensity per scan of all target lines relative to the integrated intensity per scan of the background (we call this the integrated contrast). For molecules with multiple peaks, we calculated the contrast (both peak and integrated) for each set of target and background peaks that overlap.

## RESULTS

We first tested SUCCESS on aspartate (Asp), which has a typical concentration of 3 mM in the brain. Asp contains a pair of protons, attached to a common carbon atom, with a long-lived singlet state that has previously been investigated (29). Its acetylated form, N-acetylaspartate (NAA), is present in the brain at a concentration 3–6 times higher (38–40,5). The geminal protons of interest in both molecules produce a second-order NMR spectral structure in the 2–3 ppm chemical shift range, with further splitting caused by a third nearby proton, the peak of which appears near 4 ppm (Fig. 2A–B).

In the control solutions, we measured the singlet-state lifetimes  $T_S = 5.6 \pm 1$  and  $4.5 \pm 0.3$  s for Asp and NAA, respectively, and spin–lattice relaxation times  $T_1 = 1.3 \pm 0.2$  and  $0.99 \pm 0.06$  s for the proton pairs in Asp and NAA, respectively.

Figure 2C shows that the measured one-pulse spectrum of the mixture (3.0 mM Asp, 11.4 mM NAA) is dominated by NAA and only the Asp peaks near 2.8 ppm are visible. Using an appropriate set of pulse-sequence parameters (see Fig. 2 caption), we achieved a SUCCESS spectrum (Fig. 2E) with residual NAA magnetization of only 0.7% of its original integrated intensity in the control solution. The same SUCCESS sequence applied to the Asp control produced a spectrum that appeared similar to its one-pulse spectrum, but with an integrated signal strength  $\approx 15\%$  of its original intensity (Fig. 2D). Thus the result of the SUCCESS technique was an integrated contrast enhancement  $> 20$ . Also, the aspartate peak intensities averaged 25% of their original strengths and the peak contrast enhancement due to SUCCESS was  $> 6$  for all Asp peaks compared with NAA. Importantly, the SUCCESS spectrum of the mixture (Fig. 2F) appeared nearly identical to that of the Asp control, except for the weak residual NAA signal near 2.5 ppm. Moreover, the water signal was suppressed by a factor of 6.5.

We next applied SUCCESS to the amino acid threonine (Thr), which occurs at concentrations of around 500  $\mu\text{M}$  in the brain (41,42). Threonine does not possess a pair of geminal protons, so the singlet is instead created on the vicinal protons attached

to carbons two and three. The target proton peaks lie near 3.6 and 4.2 ppm (Fig. 3A) and the down-field proton is also coupled to a methyl group ( $\delta = 1.25$  ppm), which produces a multiplet splitting pattern. We measured a singlet lifetime  $T_S = 2.0 \pm 0.3$  s and spin–lattice relaxation times  $T_1 = 2.0 \pm 0.2$  and  $2.2 \pm 0.1$  s for the vicinal protons. The singlet lifetime is shorter than  $T_1$  because the interactions with the methyl group are strongly asymmetric with respect to the singlet spins. Note that interactions with the methyl group also lead to a measured SUCCESS spectrum (Fig. 3E) that is significantly different from the one-pulse spectrum (Fig. 3A): in particular, the 4.2-ppm peak is inverted.

The up-field target proton spectral peak in Thr is overlapped by peaks from the common metabolite *myo*-inositol (spectrum shown in Fig. 3B), which occurs in the brain at concentrations of 4–12 mM (38,5). At a 10:1 *myo*-inositol:threonine concentration ratio, the *myo*-inositol peaks completely cover the up-field threonine peak and make it unresolvable in our spectrometer (Fig. 3D). Even at a 1:1 concentration ratio, the threonine peak is only partially resolved (Fig. 3C). The optimized SUCCESS sequence suppressed the *myo*-inositol peaks to less than 0.7% of their original peak intensity, while it preserved 12% of the threonine peak signal intensity (Fig. 3E–F). The result was an average peak contrast enhancement of 17. Using integrated intensities, SUCCESS recovered 15.5% of threonine signal versus 0.3% for *myo*-inositol, to produce an integrated contrast enhancement of 60. When applied to the sample with equal concentrations of threonine and *myo*-inositol, the SUCCESS sequence reduced the intensity of *myo*-inositol so greatly that only the threonine peak was evident (Fig. 3G). When performed on the sample with a 10:1 concentration ratio, the resulting spectrum exhibited a threonine peak slightly more intense than *myo*-inositol, which allowed the previously hidden peaks to be identified (Fig. 3H). Full isolation of the threonine signal was not achieved in this case because the contrast enhancement was not great enough to overcome the large concentration ratio between threonine and *myo*-inositol. The water peak was suppressed by a factor of 32.

Finally, we applied SUCCESS to a mixture of glutamine (Gln) and glutamate (Glu), which play essential roles in neurotransmission. The typical glutamate concentration is twice that of glutamine in the brain (8 and 4 mM respectively) (41,38,5,43). These molecules have largely overlapping NMR spectra, which makes molecule-specific measurements difficult (44), as well as similar chemical shifts and  $J$ -coupling strengths, which makes the application of traditional quantum filters challenging. A number of spectral-editing techniques and quantum filters have been used to attack this problem (18,19,10,45–48), but none has become a routine and reliable way to measure glutamine concentration under physiologically relevant conditions.

Each molecule contains two methylene groups that can be viewed as pairs of strongly coupled, unresolvable protons. A third lone proton couples to one of the methylene groups. The NMR spectra therefore exhibit a complex splitting pattern (Fig. 4A–B), with methylene group peaks between 1.8 and 2.6 ppm and the lone proton peak at 3.7 ppm. A mixture of the two metabolites produces a spectrum with many poorly resolved peaks and the up-field methylene groups cannot be resolved at all (Fig. 4C). Each methylene group is already strongly mixed into singlet and triplet states, but the resulting singlets cannot be easily manipulated for utilization in the SUCCESS quantum filter. Instead, a four-spin singlet state can be created by mixing the triplet states of the two methylene groups. This

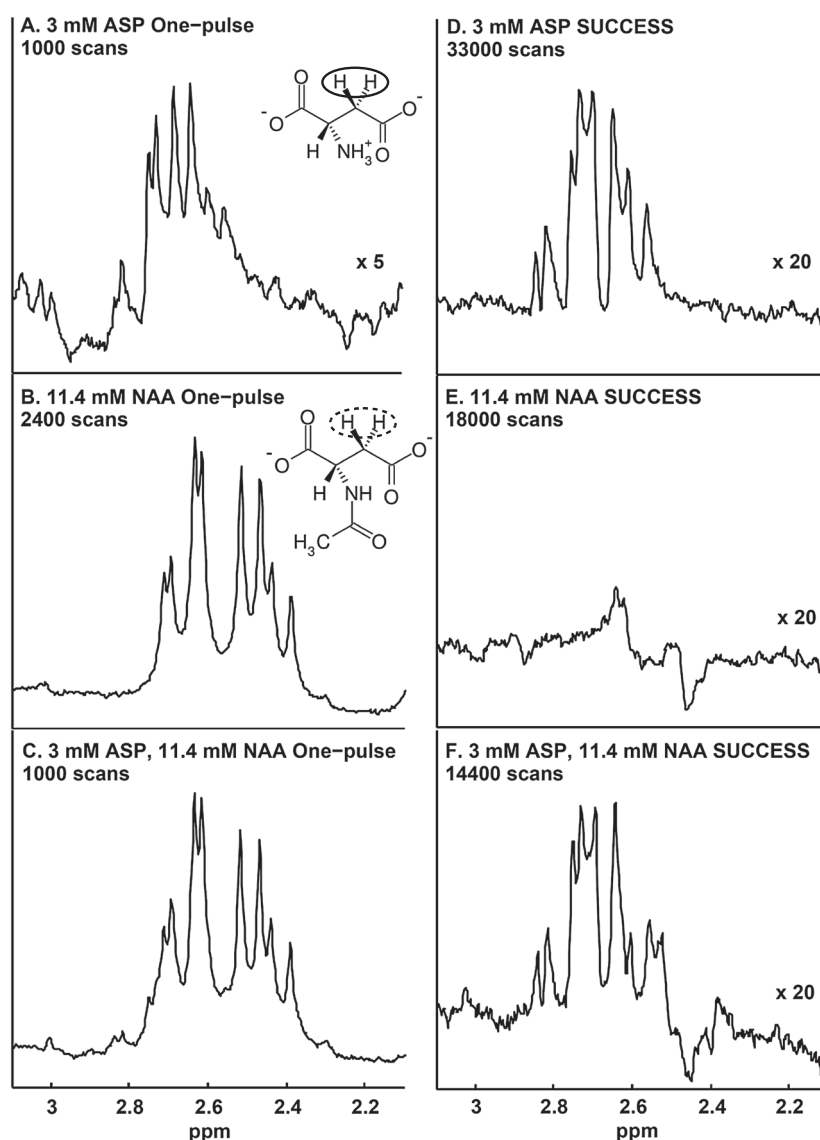


**Figure 2.** Measured NMR spectra for one-pulse (left column) and SUCCESS (right column) experiments performed on solutions of N-acetylaspartate (NAA), aspartate (Asp) and their mixture (intensity normalized by number of scans,  $N$ ). The target protons for singlet formation are indicated on each molecule, with a solid oval for Asp indicating the targeted singlet and a dashed oval for NAA indicating the undesired singlet. SUCCESS parameters were  $\delta_0 = 2.71$  ppm,  $\tau_1 = 9$  ms,  $\tau_2 = 20.3$  ms,  $\tau_3 = 11.5$  ms,  $\tau_4 = 1$  s and  $\nu_{rf} = 385$  Hz, with line broadening 0.5 Hz. The one-pulse spectra of (A) aspartate and (B) N-acetylaspartate target spins both show strong second-order structure resulting from  $J$  couplings of the same order as the resonance-frequency differences. Due to the significant structural and spectral similarity, in the one-pulse spectrum of the mixture (C), only the aspartate peaks furthest down-field are evident. (D) The SUCCESS experiment targeting aspartate produces a spectrum with a similar shape to the one-pulse experiment when applied to the aspartate solution. (E) The SUCCESS experiment produces a weak signal when performed on N-acetylaspartate solution, with only residual magnetization remaining. (F) The SUCCESS experiment produces a spectrum dominated by aspartate when performed on the mixture.

singlet is preserved by RF spin locking, just like a two-spin singlet. We found that the four-spin singlet can be selectively created depending on the pulse-sequence parameters. It still possesses spherical symmetry and passes through the polyhedral singlet filter, but it does not possess an extended lifetime. We measured lifetimes of  $0.70 \pm 0.09$  and  $0.80 \pm 0.1$  s for the four-spin singlet in glutamate and glutamine, respectively; for the two methylene group triplet states we measured  $T_1 = 1.11 \pm 0.02$  and  $0.92 \pm 0.02$  s for glutamate and  $1.24 \pm 0.05$  and  $1.01 \pm 0.04$  s for glutamine. Since the four-spin singlet state is made up of two triplet states that can undergo relaxation, the singlet-state lifetimes were shorter than the spin-lattice lifetimes of their constituent methylene groups. Nevertheless, we found that the four-spin

singlet lifetime is sufficiently long for SUCCESS to be effective in glutamine and glutamate.

We optimized the SUCCESS pulse sequence delays experimentally to obtain high contrast for glutamine. The measured SUCCESS spectrum for glutamine (Fig. 4D) was similar to the one-pulse spectrum (Fig. 4A), whereas the SUCCESS spectrum for glutamate consisted only of a single, very weak peak (Fig. 4E) compared with the intense multi-peak one-pulse spectrum (Fig. 4B). The SUCCESS spectrum of the Gln/Glu mixture (Fig. 4F) appeared similar to that of glutamine, with the small residual glutamate peak at 2.3 ppm. This residual peak did not interfere with any glutamine peaks and so the positions of the up-field methylene peaks of glutamine were now measurable. The

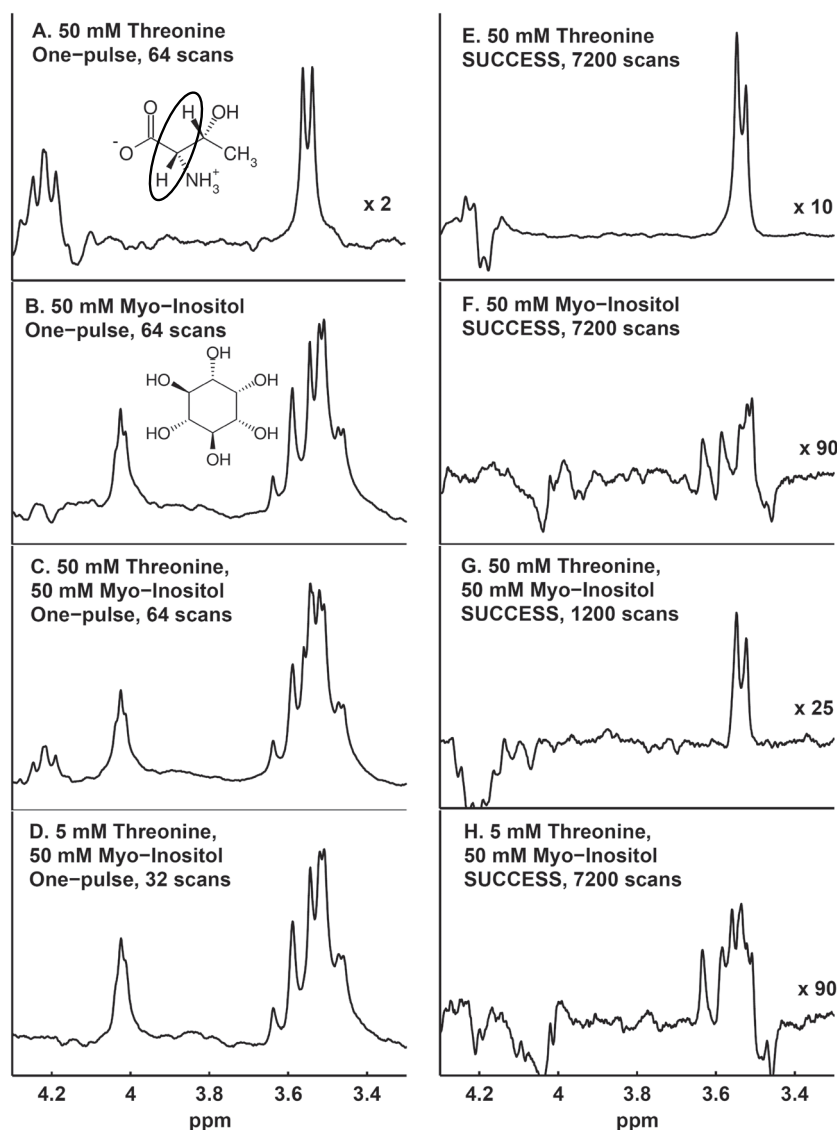


**Figure 3.** Measured NMR spectra for one-pulse (left column) and SUCCESS (right column) experiments targeting threonine performed on solutions of *myo*-inositol, threonine and two mixtures (intensity normalized by number of scans). The target protons for singlet formation on threonine are indicated by the solid oval. SUCCESS parameters were  $\delta_0 = 3.87$  ppm,  $\tau_1 = 40$  ms,  $\tau_2 = 52$  ms,  $\tau_3 = 1.85$  ms,  $\tau_4 = 200$  ms and  $\nu_n = 790$  Hz, except for frame (G), where  $\tau_2 = 72$  ms and  $\tau_3 = 4.8$  ms, with line broadening 0.5 Hz. (A) The one-pulse threonine spectrum of the target spins consists of a doublet and a multiplet. (B) The one-pulse *myo*-inositol spectrum contains a number of peaks that overlap the threonine doublet, such that in (C), a 1:1 mixture, the threonine doublet is only partially resolved and in (D), a 10:1 mixture, it is completely hidden. (E) The SUCCESS sequence produces a threonine spectrum with the same doublet, but with an inverted multiplet due to interactions with the nearby methyl group. (F) The *myo*-inositol SUCCESS spectrum with the same parameters is around 17 times weaker. (G) SUCCESS of a 1:1 mixture effectively removes the *myo*-inositol signal. (H) For a 10:1 mixture, the previously hidden threonine doublet is now partially resolved.

glutamate signal was suppressed so that only 0.5% of its original integrated intensity remained, while 5.1% of the glutamine integrated signal intensity was recovered, resulting in a Gln/Glu contrast enhancement of 10 due to SUCCESS. The peak intensities of glutamate were at most 0.86% of the original levels, while those of glutamine averaged 5.7% of the original intensity, thereby producing peak Gln/Glu contrast enhancements between 3 and 7. The water signal was suppressed by a factor of 13.

The transmitter frequency can also be used as a parameter to optimize SUCCESS contrast. We found that a higher signal from glutamine could be obtained by moving the transmitter frequency approximately 40 Hz up-field from the average value, to  $\delta_{\text{mav}} = 2.05$  ppm, for the whole sequence and by applying a

different set of delays. This frequency adjustment created the same level of peak contrast while preserving 15% of the glutamine peak signal intensity (see the Supplementary Material, Fig. S1A–C). Water suppression was also higher, with a peak 38 times weaker than in a one-pulse scan.

While SUCCESS is designed to be effective at removing background signals in the same spectral region as a target, it is less effective at removing signals spectrally far from the target. We performed measurements on the suppression of the water peak in buffer solution alone, using parameters for glutamine, and found that the SUCCESS filter has a bandwidth of approximately 250 Hz. Outside this bandwidth, background suppression varies, which may lead to significant differences in water

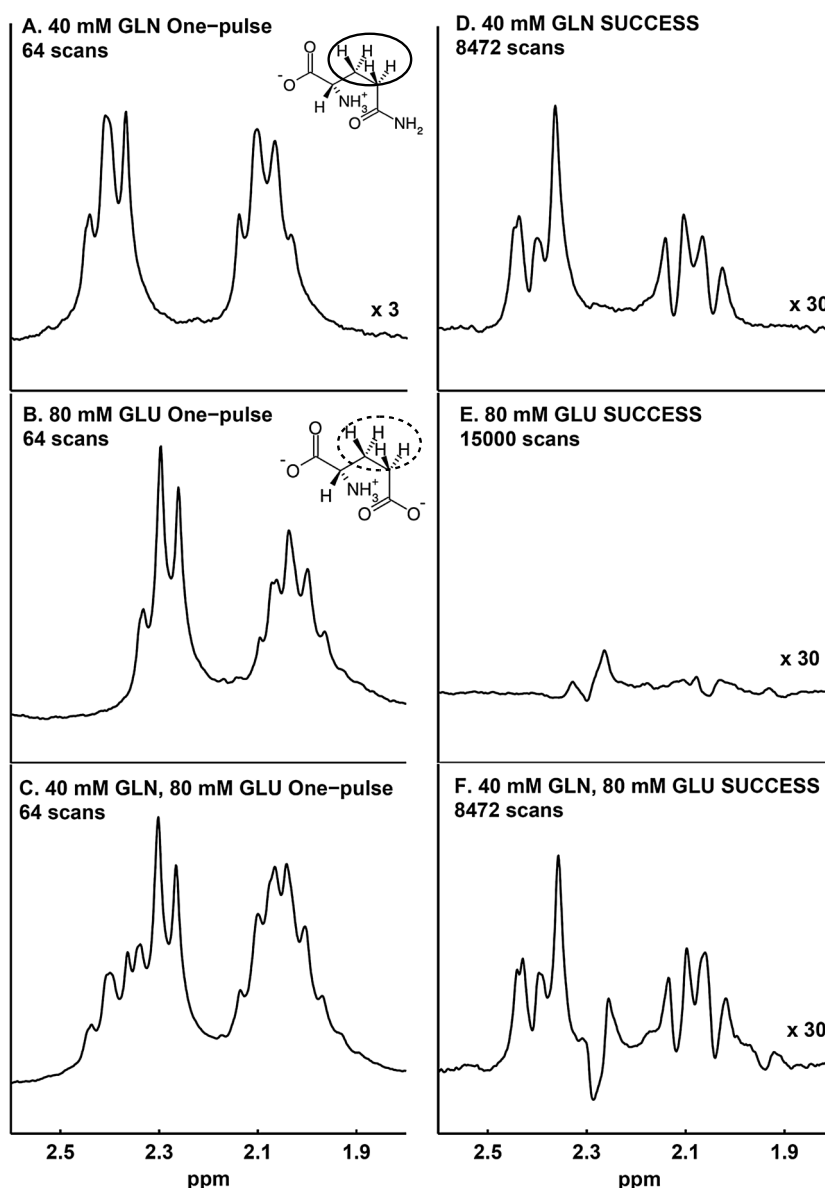


**Figure 4.** Measured NMR spectra for one-pulse (left column) and SUCCESS (right column) experiments targeting glutamine performed on solutions of glutamate (Glu), glutamine (Gln) and their mixture (intensity normalized by number of scans). The protons for singlet formation are indicated on each structure, with a solid oval indicating the targeted singlet spins for glutamine and a dashed oval indicating the undesired singlet for glutamate. SUCCESS parameters were  $\delta_0 = 2.23$  ppm,  $\tau_1 = 22$  ms,  $\tau_2 = 15$  ms,  $\tau_3 = 11.1$  ms,  $\tau_4 = 500$  ms and  $\nu_n = 385$  Hz, with line broadening 1 Hz. The one-pulse spectra of (A) glutamine and (B) glutamate both exhibit a complex structure with similar chemical shifts. In the spectrum of (C), the mixture, the glutamine peaks near 2.4 ppm are partially resolved while those near 2.1 ppm are unresolved from those of glutamate. The SUCCESS spectrum of (D) glutamine is similar in structure to the one-pulse spectrum, whereas that of (E) glutamate contains only weak residual peaks. The SUCCESS spectrum of (F), the mixture, is similar to that of glutamine alone, except for a residual glutamate signal near 2.3 ppm.

suppression for different metabolites. It may be possible to develop a more broad-band filter using magnetic gradients in lieu of the phase cycle to act as a dephasing mechanism for spins not in the singlet state.

## DISCUSSION

We have demonstrated the use of nuclear spin singlet states as a new mechanism for contrast enhancement using quantum filtration. We emphasize that the singlet state is related to quantum coherences previously utilized as filters. For instance,

double-quantum (DQ) and zero-quantum (ZQ) coherences have been used extensively for a large number of quantum-filter and spectral-editing applications. However, the singlet state has unique requirements for its creation and preservation that give SUCCESS greater selectivity. The sensitivity of the pulse sequence to spectral parameters shares properties with both zero-quantum and double-quantum filters. As in each of these, two SUCCESS delays are matched to the  $J$  coupling. However, SUCCESS is sensitive to both the sum of the resonance frequencies  $\Sigma\omega$ , like a DQ filter, and the difference in resonance frequencies  $\Delta\omega$ , like a ZQ filter (6,14). In fact, two sequence timings are matched to  $\Delta\omega$ , rather than only one in a ZQ filter.

**Table 2.** Comparison of delay dependence on spectral parameters for SUCCESS, double (DQ) and zero (ZQ) quantum filters

Parameter	SUCCESS	DQ	ZQ
$\tau_1$	$J$	$J$	$J$
$\tau_2$	$J, \Delta\omega, \Sigma\omega$	$J$	$J$
$\tau_3$	$\Delta\omega$	—	—
Evolution time ( $t$ )	$\Delta\omega, \Sigma\omega$	$\Sigma\omega$	$\Delta\omega$

Like ZQ filters, SUCCESS has an advantage over DQ filters when the average frequency of the spins is nearly the same in the target and the background, since in such a case  $\Sigma\omega$  is nearly identical. Like a DQ filter, SUCCESS is sensitive to transmitter frequency and field inhomogeneities. If the third pulse is replaced with a 45° pulse, both this sensitivity and a source of control are removed (22). This may be necessary for use in biological systems such as the brain, where differences in susceptibility lead to line shifts and line broadening. In fact, these effects increase with magnetic field strength and make MRS more difficult, so it is beneficial for the SUCCESS quantum filter to work well at relatively low magnetic fields. Table 2 compares the three filters.

In SUCCESS, the preservation of the singlet also requires RF power to be applied at a proper resonance frequency and at a sufficient intensity (31,22,21,49). To preserve the singlet properly, the RF spin-locking frequency should also be at least five times higher than the resonance-frequency difference between target spins (31). By using weaker spin locking, singlets in molecules with widely separated spectral peaks (large  $\Delta\omega$ ) can be rejected in favour of those with more closely spaced peaks. Additionally, since frequency differences due to chemical shift decrease as  $B_0$  is lowered, lower field spectrometers can use weaker spin-locking fields, resulting in lower RF specific absorption rates (SAR) (31). It may also be possible to reduce the length of spin locking and allow phase cycling to provide most of the filtering.

We note that the requirements for good singlet-state purity also limit the efficiency of the SUCCESS technique. As the target nuclear-spin pair is coupled to more surrounding spins in a molecule, the efficiency of singlet creation decreases, as well as the singlet purity. In an ideal spin pair, at most 50% of the magnetization can be transferred to the singlet state, while the other half is transferred to the triplet states and is lost. For example, in aspartate the coupling strength to the third proton is around half the coupling strength between the target spins, so that nearly 50% transfer can still be achieved. However, in threonine, coupling with the neighboring methyl group is stronger than the coupling between the target protons, leading to a mixture of the singlet state with the methyl group states. Simulations show that the maximum amount of magnetization transferred to the singlet is reduced to 25%. It may be possible to improve singlet production in the future using more complex preparation sequences that remove the effects of these attached spins, so that there is a lower loss of sensitivity.

We should also consider that the highest target/background contrast is not always achieved with SUCCESS parameters that produce maximal target intensity. For example, *myo*-inositol contains an even number of protons that can form states with some singlet character and the best contrast for threonine is achieved when the delays minimize the amount of *myo*-inositol

singlet created. However, with these parameters only 20% of the threonine magnetization is transferred into the singlet state. Moreover, RF power must remain on for a sufficiently long time to let the system evolve and saturate the triplet states. During this time, there is some singlet relaxation. These various magnetization losses mean that the contrast improvements afforded by SUCCESS come with a trade off in experiment time or imaging resolution. Using delays optimized for best singlet creation, the SUCCESS sequence requires at least four times as many scans, or voxels of twice the volume, to achieve the same signal-to-noise ratio as one-pulse scans. Similar sensitivity losses are common in most multiple-quantum filters (46,9,11). The extra number of scans might be a drawback of SUCCESS for *in vivo* application, especially due to the time required for spin locking and  $T_1$  recovery, and may preclude human use unless these delays can be sufficiently reduced.

In summary, we demonstrated experimentally that the SUCCESS quantum filtration technique, which utilizes nuclear spin singlet states, can create strong and specific contrast enhancement in NMR spectroscopy, e.g. improving the measurement of brain metabolites such as glutamine. Moreover, this work highlights the ubiquity of singlet states and demonstrates a key singlet-state application beyond extended spin lifetimes. We expect the SUCCESS technique to find application in NMR-based measurements of biosamples to aid in the diagnosis of disease without resorting to increasingly high-field spectrometers. With future improvements, it might also be applied to animal and human MRS measurements.

## Acknowledgement

We acknowledge support from the National Science Foundation (NSF).

## REFERENCES

- Wevers RA, Engelke U, Heershap A. High-resolution 1H-NMR spectroscopy of blood plasma for metabolic studies. *Clin. Chem.* 1994; 40: 1245–1250.
- Zuppi C, Messana I, Forni F, Rossi C, Pennacchietti L, Ferrari F, Giardina B. <sup>1</sup>H NMR spectra of normal urines: Reference ranges of the major metabolites. *Clin. Chim. Acta* 1997; 265: 85–97.
- Coen M, Holmes E, Lindon JC, Nicholson JK. NMR-based metabolic profiling and metabonomic approaches to problems in molecular toxicology. *Chem. Res. Toxicol.* 2008; 21: 9–27.
- Soares DP, Law M. Magnetic resonance spectroscopy of the brain: review of metabolites and clinical applications. *Clin. Radiol.* 2009; 64: 12–21.
- Ross B, Bluml S. Magnetic resonance spectroscopy of the human brain. *Anat. Rec. (New Anat.)* 2001; 265: 54–84.
- Ernst RR, Bodenhausen G, Wokaun A. *Principles of Nuclear Magnetic Resonance in One and Two Dimensions*. Oxford University Press: Oxford; 1987.
- Dumoulin CL, Vatis D. Water suppression in 1H magnetic resonance images by the generation of multiple-quantum coherence. *Magn. Reson. Med.* 1986; 3: 282–288.
- Star-Lack JM, Spielman DM. Zero-quantum filter offering single-shot lipid suppression and simultaneous detection of lactate, choline, and creatine resonances. *Magn. Reson. Med.* 2001; 46: 1233–1237.
- Lei H, Peeling J. A localized double-quantum filter for *in vivo* detection of taurine. *Magn. Reson. Med.* 1999; 42: 454–460.
- Thompson RB, Allen PS. A new multiple quantum filter design procedure for use on strongly coupled spin systems found *in vivo*: Its application to glutamate. *Magn. Reson. Med.* 1998; 39: 762–771.
- Wilman AH, Allen PS. *In vivo* NMR detection strategies for  $\gamma$ -aminobutyric acid, utilizing proton spectroscopy and coherence-pathway filtering with gradients. *J. Magn. Reson., Ser. B* 1993; 101: 165–171.

12. de Graaf RA, Rothman DL, Behar KL. High resolution NMR spectroscopy of rat brain *in vivo* through indirect zero-quantum-coherence detection. *J. Magn. Reson.* 2007; 187: 320–326.
13. Doddrell DM, Brereton IM. A selective excitation/ $B_0$  gradient technique for high-resolution  $^1\text{H}$  NMR studies of metabolites via zero-quantum coherence and polarization transfer. *NMR Biomed.* 1989; 2: 39–43.
14. Dijk JE, Mehlkopf AF, Boveé WMMJ. Comparison of double and zero quantum NMR editing techniques for *in vivo* use. *NMR Biomed.* 1992; 5: 75–86.
15. Rance M, Dalvit C, Wright PE. Simplification of  $^1\text{H}$  NMR spectra of proteins by one-dimensional multiple quantum filtration. *Biochem. Biophys. Res. Commun.* 1985; 131: 1094–1102.
16. Cavanagh J, Fairbrother WJ, Palmer AG III, Rance M, Skelton NJ. *Protein NMR Spectroscopy: Principles and Practice.* Academic Press: Amsterdam; 2006.
17. Müller N, Ernst RR, Wüthrich K. Multiple-quantum-filtered two-dimensional correlated NMR spectroscopy of proteins. *J. Am. Chem. Soc.* 1986; 108: 6482–6492.
18. Snyder SR, Kirsch S, Kraus K, Bachert P. Two-dimensional zero-quantum coherence  $^1\text{H}$  NMR spectroscopy of glutamate and glutamine. *Proc. Int. Soc. Magn. Reson. Med.* 2008; 16: 1564.
19. Thompson RB, Allen PS. Response of metabolites with coupled spins to the STEAM sequence. *Magn. Reson. Med.* 2001; 45: 955–965.
20. Farkas A. *Orthohydrogen, Parahydrogen, and Heavy Hydrogen.* Cambridge University Press: Cambridge; 1935.
21. Pileio G, Levitt MH. Theory of long-lived nuclear spin states in solution nuclear magnetic resonance. II. Singlet spin locking. *J. Chem. Phys.* 2009; 130: 214501.
22. Levitt MH. Singlet and other states with extended lifetimes. *Encyclopedia of Magnetic Resonance.* John Wiley & Sons: Chichester, UK; 2010.
23. Gopalakrishnan K, Bodenhausen G. Lifetimes of the singlet-states under coherent off-resonance irradiation in NMR spectroscopy. *J. Magn. Reson.* 2006; 182: 254–259.
24. Pileio G, Concistré M, Carravetta M, Levitt MH. Long-lived nuclear spin states in the solution NMR of four-spin systems. *J. Magn. Reson.* 2006; 182: 353–357.
25. Carravetta M, Johannessen O, Levitt MH. Beyond the T1 limit: Singlet nuclear spin states in low magnetic field. *Phys. Rev. Lett.* 2004; 92: 153003.
26. Carravetta M, Levitt MH. Long-lived nuclear spin states in high-field solution NMR. *J. Am. Chem. Soc.* 2004; 126: 6228–6229.
27. Pileio G, Carravetta M, Hughes E, Levitt MH. The long-lived singlet state of  $^{15}\text{N}$ -nitrous oxide in solution. *J. Am. Chem. Soc.* 2008; 130: 12 582–12 583.
28. Ghosh RK, Kadlecik SJ, Ardenjaer-Larsen JH, Pullinger BM, Pileio G, Levitt MH, Kuzma NN, Rizi RR. Measurements of the persistent singlet state of  $\text{N}^2\text{O}$  in blood and other solvents—potential as a magnetic tracer. *Magn. Reson. Med.* 2011; 66: 1177–1180.
29. Vasos PR, Comment A, Sarkara R, Ahuja P, Jannin S, Ansermet JP, Konter JA, Hautle P, van den Brandt B, Bodenhausen G. Long-lived states to sustain hyperpolarized magnetization. *Proc. Natl. Acad. Sci. USA* 2009; 106: 18 469–18 473.
30. Ahuja P, Sarkar R, Vasos PR, Bodenhausen G. Long-lived states in multiple-spin systems. *Chemphyschem* 2009; 10: 2217–2220.
31. DeVience SJ, Walsworth RL, Rosen MS. Dependence of nuclear spin singlet lifetimes on RF spin-locking power. *J. Magn. Reson.* 2012; 218: 5–10.
32. Sarkar R, Vasos PR, Bodenhausen G. Singlet-state exchange NMR spectroscopy for the study of very slow dynamic processes. *J. Am. Chem. Soc.* 2006; 129: 328–334.
33. Sarkar R, Ahuja P, Vasos PR, Bodenhausen G. Measurement of slow diffusion coefficients of molecules with arbitrary scalar couplings via long-lived spin states. *Chemphyschem* 2008; 9: 2414–2419.
34. Cavadini S, Dittmer J, Antonijevic S, Bodenhausen G. Slow diffusion by singlet state NMR spectroscopy. *J. Am. Chem. Soc.* 2005; 127: 15 744–15 748.
35. Warren WS, Jenista E, Branca RT, Chen X. Increasing hyperpolarized spin lifetimes through true singlet eigenstates. *Sci.* 2009; 323: 1711–1714.
36. Pileio G, Levitt MH. Isotropic filtering using polyhedral phase cycles: Application to singlet state NMR. *J. Magn. Reson.* 2008; 191: 148–155.
37. Levitt MH. SpinDynamica code for Mathematica. Website title: SpinDynamica: Magnetic Resonance in Mathematica, 2011. Available at <http://www.SpinDynamica.soton.ac.uk> (Accessed May 18, 2011).
38. Cudalbu C, Cavassila S, Ratiney H, Beuf O, van Ormondt D, Graveron-Demilly D. Metabolite concentration estimates in the rat brain by magnetic resonance spectroscopy using QUEST and two approaches to invoke prior knowledge. *IEEE Proc. ProRISC, Veldhoven, Neth.* 2005; 609–614.
39. Sarchielli P, Presciutti O, Pelliccioli GP, Tarducci R, Gobbi G, Chiarini P, Alberti A, Vicinanza F, Gallai V. Absolute quantification of brain metabolites by proton magnetic resonance spectroscopy in normal-appearing white matter of multiple sclerosis patients. *Brain* 1999; 122: 513–521.
40. Birken DL, Oldendorf WH. N-acetyl-L-aspartic acid: A literature review of a compound prominent in  $^1\text{H}$ -NMR spectroscopic studies of brain. *Neurosci. Biobehav. Rev.* 1989; 13: 23–31.
41. Wallwork JC, Sandstead HH. Effect of zinc deficiency on appetite and free amino acid concentrations in rat brain. *J. Nutr.* 1983; 113: 47–54.
42. Choi C, Coupland NJ, Kalra S, Bhardwaj PP, Malykhin N, Allen PS. Proton spectral editing for discrimination of lactate and threonine 1.31 ppm resonances in human brain *in vivo*. *Magn. Reson. Med.* 2006; 56: 660–665.
43. Schubert F, Gallinat J, Seifert F, Rinneberg H. Glutamate concentrations in human brain using single voxel proton magnetic resonance spectroscopy at 3 Tesla. *Neuroimage* 2004; 21: 1762–1771.
44. Mason GF, Pan JW, Ponder SL, Twieg DB, Pohost GM, Hetherington HP. Detection of brain glutamate and glutamine in spectroscopic images at 4.1 T. *Magn. Reson. Med.* 1994; 32: 142–145.
45. Choi C, Coupland NJ, Bhardwaj PP, Malykhin N, Gheorghiu D, Allen PS. Measurement of brain glutamate and glutamine by spectrally-selective refocusing at 3 Tesla. *Magn. Reson. Med.* 2006; 55: 997–1005.
46. Hu J, Yang S, Xuan Y, Jiang Q, Yang Y, Haake EM. Simultaneous detection of resolved glutamate, glutamine, and  $\gamma$ -aminobutyric acid at 4 T. *J. Magn. Reson.* 2007; 185: 204–213.
47. Lee HK, Yaman A, Nalcioğlu O. Homonuclear J-refocused spectral editing technique for quantification of glutamine and glutamate by  $^1\text{H}$  NMR spectroscopy. *Magn. Reson. Med.* 1995; 34: 253–259.
48. Yang S, Hu J, Kou Z, Yang Y. Spectral simplification for resolved glutamate and glutamine measurement using a standard STEAM sequence with optimized timing parameters at 3, 4, 4.7, 7, and 9.4 T. *Magn. Reson. Med.* 2008; 59: 236–244.
49. Pileio G. Relaxation theory of nuclear singlet states in two spin-1/2 systems. *Prog. Nucl. Magn. Reson. Spectrosc.* 2010; 56: 217–231.